Effect of high pressure on the crystal structures of polymorphs of glycine

Cite as:
Dawson, A., Allan, D. R., Belmonte, S. A., Clark, S. J., David, W. I. F., McGregor, P. A., Parsons, S., Pulham, C. R., & Sawyer, L. (2005). Effect of high pressure on the crystal structures of polymorphs of glycine. *Crystal Growth & Design*, 5(4), 1415-1427.

Manuscript received: 14/08/2004; Revised: 03/04/2005; Article published: 06/07/2005

Effect of High Pressure on the Crystal Structures of Polymorphs of Glycine**

Alice Dawson,[1] David R. Allan,[1] Scott A. Belmonte,[2] Stewart J. Clark,[3] William I.F. David,[4] Pamela A. McGregor,[2] Simon Parsons,[1,*] Colin R. Pulham[1] and Lindsay Sawyer[5]

[1]EaStCHEM, School of Chemistry Centre for Science at Extreme Conditions, Joseph Black Building, University of Edinburgh, West Mains Road, Edinburgh, EH9 3JJ, UK.

[2]School of Physics and Astronomy and Centre for Science at Extreme Conditions, The University of Edinburgh, King's Buildings, West Mains Road, Edinburgh, Scotland, EH9 3JZ, UK.

[3]Department of Physics, University of Durham, South Road, Durham, England, DH1 3LE, UK.

[4]ISIS Facility, Rutherford Appleton Laboratory, Didcot, Oxfordshire, England, OX11 0QX, UK.

[5]Institute for Cell and Molecular Biology and Centre for Science at Extreme Conditions, The University of Edinburgh, King's Buildings, West Mains Road, Edinburgh, Scotland, EH9 3JR.

[*]Corresponding author; S.P. e-mail: S.Parsons@ed.ac.uk, tel: +44 131 650 4804, fax: +44 131 650 4743

[**]We thank the EPSRC and The University of Edinburgh for funding and the CCLRC for provision of synchrotron beam-time, some of which was made available through the DARTS service. We also thank Prof. R.J. Nelmes and Dr. M.I. McMahon (both University of Edinburgh) for the use of their equipment on Station 9.1 at Daresbury SRS and Drs Simon Teat and Alistair Lennie (CCLRC Daresbury Laboratory) for their valuable help with the data collections on Stations 9.8 and 9.1. We also thank Dr A. Kern of Bruker-Nonius for a copy of TOPAS3, and Dr A. Coelho for his help with the Rietveld refinements.

Graphical abstract

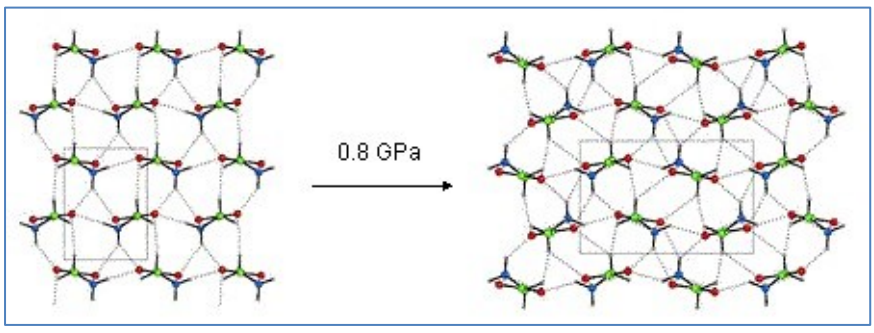

Supporting information:

Crystallographic information files (cif) are available free of charge via the Internet at http://pubs.acs.org

Abstract

The effect of high pressure on the crystal structures of α-, β- and γ-glycine has been investigated. A new polymorph, δ-glycine, is obtained from β glycine. δ-Glycine is monoclinic, $P2_1/a$, a = 11.156(4), b = 5.8644(11), c = 5.3417(17) Å, β = 125.83(4)° at 1.9 GPa. The transition, which occurs between 0 and 0.8 GPa, proceeds from a single crystal of β-glycine to a single crystal of δ-glycine, resulting in an equal number of NH…O hydrogen bonds, but an increase in the number and strength of CH…O hydrogen bonds, which act to close-up of 'holes' which are formed within the layers of β-glycine in the centers of *R*-type hydrogen bonded motifs. Trigonal γ-glycine begins to undergo a transition to another high-pressure phase, ε-glycine, at 1.9 GPa, but the transformation is destructive; it is essentially complete at 4.3 GPa. The structure is monoclinic *Pn*, a = 4.8887(10), b = 5.7541(11), c = 5.4419(11) Å, β = 116.682(10)° at 4.3 GPa. The structure consists of layers similar those observed in α-glycine with inter-layer separations of 2.38 and 3.38 Å and CH…O interactions formed between the layers. Monoclinic α-glycine is known to be stable to 23 GPa, and we have obtained a single crystal structure of this polymorph at 6.2 GPa. Super-short NH…O hydrogen bonds are *not* formed up to 6.2 GPa, and they only shorten significantly if they are formed parallel to CH…O hydrogen bonds which strengthen, or vectors across holes which close-up, under pressure.

Introduction

There have been several recent studies on the effects of high pressure on organic molecular systems[1,2] and proteins.[3-5] These are of current interest in areas such as pressure-treatment of food products and the study of extremophile bacteria that live in the deep oceans and the Earth's crust. Computational approaches to this problem are hampered by the lack of structural data that can be used in the development of inter-residue potential functions. The parameters suitable for modelling[6,7] and refining[8] crystal structures under ambient conditions have been derived from the crystal structures of the amino acids. We have recently described the crystal structure of the amino acid *L*-serine as a function of high pressure, showing that it undergoes a transition to a new high pressure polymorph at *ca* 5 GPa. Several amino acids have also been the subject of Raman studies at high pressure.[10-13] In this paper we describe the effect of high pressure on the simplest amino acid, glycine.

Glycine has three polymorphs under ambient conditions, termed α-, β- and γ. The form obtained by evaporation of aqueous solutions is monoclinic α-glycine ($P2_1/n$).[14-18] The most stable form at ambient temperature and pressure, however, is γ-glycine,[19] which crystallizes from acidified aqueous solution in space group $P3_1/P3_2$.[18,20,21] Some fascinating recent work has shown that formation of γ-glycine from aqueous solution may also be induced by polarized laser irradiation.[22-24] The α-form has a structure based on dimers, and its prevalence is thought to be the result of the presence of dimers in solution, which lead to its

preferential nucleation.[25] Crystallisation of glycine from water/ethanol leads to formation of another monoclinic ($P2_1$) polymorph, β-glycine. At ambient pressure and temperature the order of stability is γ > α > β.[19,27]

Transformations between the α, β and γ polymorphs have been studied in detail. The γ-form transforms to the α-form on heating to around 170°C, the precise temperature depending on a variety of factors including the thermal history of the sample.[19,28] The α-to-γ transformation occurs at high humidity.[29] The β-form transforms rapidly to the α- or γ- forms in the presence of moisture at room temperature, but it is metastable in dry air.[21,30]

In this paper we describe the effect of high pressure on the α, β and γ polymorphs of glycine at ambient temperature. The effect of pressure on the α and β-polymorphs have been studied by Raman spectroscopy. While the α-phase is stable to 23 GPa,[10a] the β-form has been shown to undergo a phase transition at 0.76 GPa.[10b] The effect of pressure on a mixture of α and γ glycine was studied by Boldyreva and co-workers up to 4.0 GPa by powder diffraction.[31] The α-form persisted up to 4.0 GPa, consistent with the earlier Raman study. The lines attributable to γ-glycine were observed to 'fall-down' at 4.0 GPa. In a later study the same workers studied the effect of pressure on a powdered sample of pure γ-glycine.[32] In this study powder lines were observable up to 7.85 GPa, the highest pressure attained in the study. A transition to a new phase of glycine began to occur at 2.74 GPa. A structure of the new phase was proposed on the basis of the data obtained at 7.85 GPa.

In this paper we describe the crystal structure of α-glycine at 6.2 GPa; use single X-ray crystal diffraction allows the changes on compression to be characterized in detail. We also describe the crystal structure of the phase obtained by compression of β-glycine; this is a new phase of glycine, hereafter designated δ-glycine.[33] We show that single crystals of γ-glycine do not survive compression above 1.9 GPa. We have also obtained powder diffraction data on a sample of polycrystalline γ-glycine exposed to a pressure of 4.3 GPa, and we observe similar behaviour to that described by Boldyreva.[32] Hereafter we designate the phase obtained on compression of γ-glycine as ε-glycine, and we describe an alternative model of the structure of this phase.

We show that one of the consistent features observed on application of pressure to the different polymorphs of glycine is compression of voids in the structure together with an increase in CH…O hydrogen bonding. The characteristics of weak hydrogen bonds have been reviewed by Desiraju and Steiner,[34] while they have been surveyed in amino acids by Jeffrey and Maluszynska[35] and in proteins by Derewenda *et al*.[36] The α-hydrogen atoms in amino acids are activated towards CH…O bonding by the neighbouring nitrogen atom; the lower limit for $C_\alpha H$…O distances, as determined by neutron diffraction, is 2.16 Å, though values around 2.4 Å are more common.[35] These interactions are therefore longer than for more conventional hydrogen bonds, *e.g.* NH…O. In proteins CH…O interactions commonly occur in β-sheets, where they support medium-strength

N-H…O interactions, but they have also been shown to have a functional role in some proteins.[36] The energy of a CH…O hydrogen bond is only a few kJ mol^{-1}, but the cumulative effect of many such interactions is significant, and the suggestion has been made that they compensate for the loss of conventional hydrogen bonding incurred during protein folding. The denaturation of proteins under pressure has been ascribed to the movement of water into hydrophobic regions of the structure;[37] our results suggest that changes in the number of voids and CH…O interactions are potentially also significant.

Experimental

Single Crystal Diffraction: General Procedures

High-pressure experiments were carried out using a Merrill-Bassett diamond-anvil cell[38] equipped with 600 μm culet-cut diamonds and a tungsten gasket with a 300 μm hole. Backing disks were made from beryllium (which is polycrystalline). A 4:1 mixture of methanol and ethanol was used as the pressure transmitting medium, which ensures that pressure is applied hydrostatically.[39] A small chip of ruby was also loaded into the cell to enable pressure measurement by the ruby fluorescence method;[40] these measurements were carried-out by excitation with a 441.4 nm line from a Hg-Cd laser, the fluorescence being detected with a Jobin-Yvon LabRam 300 Raman spectrometer.

X-ray diffraction data were collected for α-glycine at room-temperature using synchrotron radiation (λ = 0.6843 Å) on the Bruker SMART diffractometer on Station 9.8 at CCLRC Daresbury Laboratory.[41] In the cases of β and γ-glycine diffraction data were collected at room-temperature on a Bruker Smart Apex diffractometer with a sealed-tube Mo-Kα source (λ = 0.71073 Å). Data were collected in ω-scans in eight settings of 2θ and ϕ; full details of data collection and processing procedures used in our laboratory have been given previously.[42] The program used for integration was SAINT,[43] and absorption corrections were carried out in a two-stage procedure using SHADE[44] and SADABS.[45]

All refinements were carried out *versus* $|F|^2$ using all data (CRYSTALS).[46] Refinements of the compressed α, β and γ phases were carried out starting from the published coordinates determined at ambient pressure. The completeness of data sets collected at high pressure on samples which belong to low-symmetry crystal systems is invariably quite low, and for this reason the primary bond distances and angles were restrained to the values observed in α-glycine at ambient pressure (restraints are listed in the cifs which form part of the supplemental data to this paper). The assumption is therefore made that primary bond distances and angles are not greatly affected at pressures up to 6.2 GPa (the highest pressure used in this study). In order to maintain a reasonable data-to-parameter ratio during refinement carbon, nitrogen and oxygen atoms were refined with isotropic displacement parameters. Hydrogen atoms were included in idealized positions.

Crystal structures were visualized using the programs XP,[47] CAMERON[48] and MERCURY.[49] Analyses were carried out using PLATON,[50] as incorporated in the WIN-GX suite.[51] Calculation of strain tensors was accomplished using a locally-written program.[52] Topological calculations were performed with TOPOS4.0.[53] Searches of the Cambridge Structural Database were carried out with the program CONQUEST,[54,55] utilising version 5.25 of the database. The numbering scheme used in this paper follows that of CSD refcode GLYCIN29, Boldyreva's room-temperature structure determination of α-glycine (Scheme 1).[18]

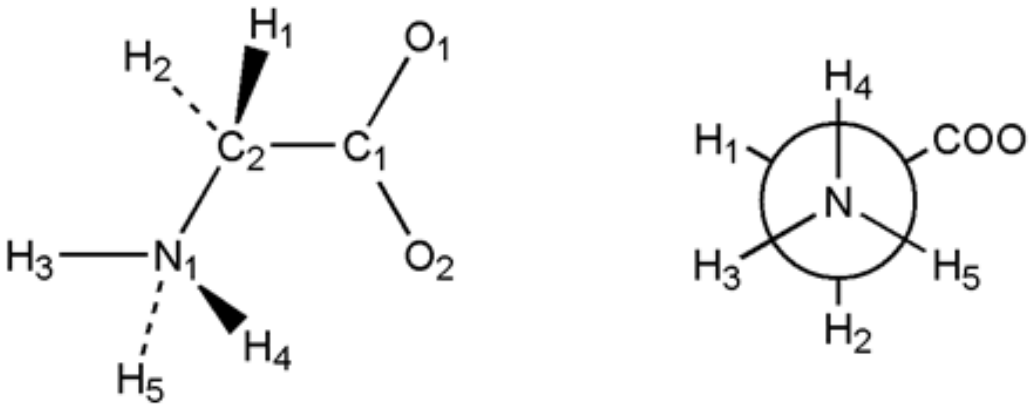

Scheme 1. Numbering scheme.

Crystal Growth

Crystals of α-glycine were grown by slow evaporation of an aqueous solution of glycine (obtained from Aldrich).[15,17] β-Glycine was obtained by slow diffusion of ethanol into a concentrated aqueous solution of glycine.[30] Crystals of γ-glycine were grown from an aqueous solution of glycine acidified with a small amount of acetic acid.[18] The identity of all phases was established by determination of the unit cell dimensions by single crystal X-ray diffraction. The crystal sample used in each of these determinations was the same as that used for the pressure study.

The compression of α-glycine studied by single crystal X-ray diffraction

Diffraction data for α-glycine were collected using synchrotron radiation (see above) at 2.0 and 6.2 GPa. The low divergence of synchrotron radiation means that the broad powder rings, which arise from the beryllium windows of the Merrill-Bassett cell, are much more highly textured ('spottier') than in data-sets collected on a home-source (see Figure 1). The most intense Be diffraction ring (from the {011} reflections) was masked-out during integration.[42,56] Eight reflections were identified as outliers (with $F_o^2 >> F_c^2$) during refinement, and the images checked to determine the source of the disagreement. In all cases some or all predicted spot positions

for a given set of symmetry-equivalent reflections overlapped with a region of high texture, usually in the {110} and {013} rings. These measurements were deleted from the data-set.

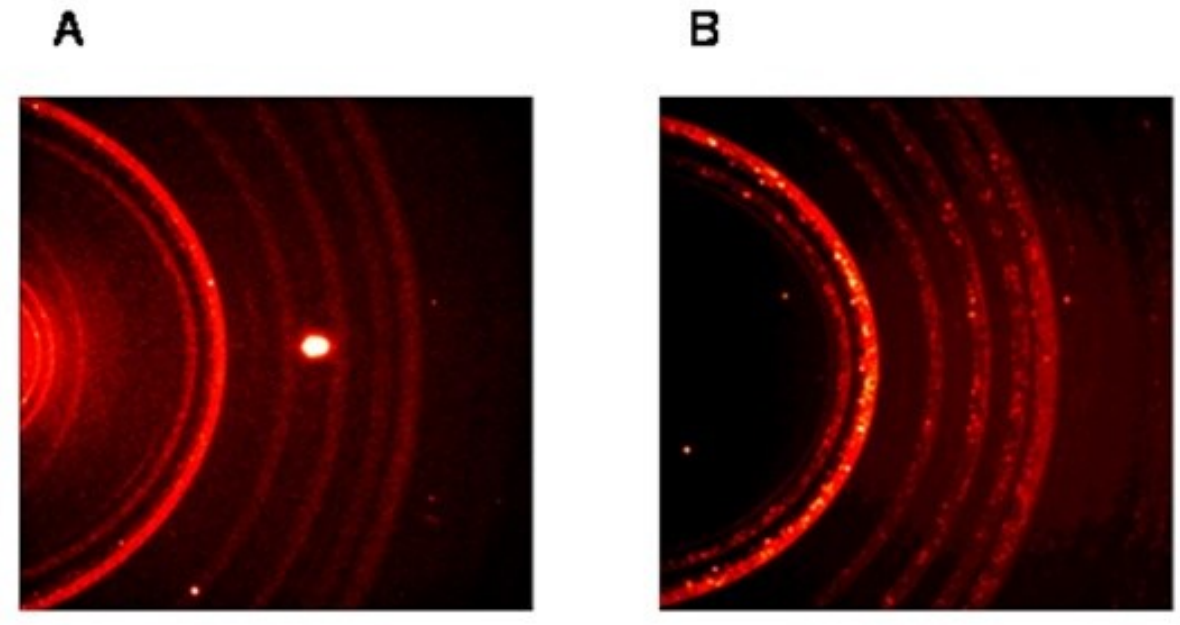

Figure 1. Data collection frames collected on α-glycine on a laboratory source (*a*) and with synchrotron radiation (*b*). The diffuse arcs are Debye-Scherrer rings from the beryllium backing plates of the pressure cell. Note that they are much more textured in (*b*). The bright spot in the center of (*a*) is a diamond reflection.

The compression of β-glycine studied by single crystal X-ray diffraction

Crystals of β-glycine are known to transform quickly to α-glycine in the presence of moisture,[26,30] and the sample was therefore loaded quickly into the pressure cell. Once inside the cell, surrounded by the hydrostatic medium, the phase was stable. Diffraction data were collected at near ambient pressure (to establish the starting phase); the cell dimensions were: monoclinic, a = 5.088(4), b = 6.266(3), c = 5.390(3) Å, β = 113.11(6)° (*cf* Table 1). Data were then collected at 0.8 and 1.9 GPa.

Determination of the cell dimensions at 0.8 GPa showed that a single-crystal to single-crystal phase transition had occurred to a new polymorph, δ-glycine. However, the phase transition appeared to have dislodged the crystal from its previously stable position in the cell, and it moved during data collection at 0.8 GPa; this meant that useful data were only obtained from six out of the eight data collection runs. The identity of the phase at 0.8 GPa is established by its cell dimensions: monoclinic, a = 11.333(8), b = 6.010(2), c = 5.379(3) Å, β = 126.13(7)°, V = 296.0(3) Å^3 (*cf* Table 1); refinement of the coordinates of the 1.9 GPa model presented here (see below) against the 0.8 GPa data set converged with $R1$[based on F and 100 data with $F>4\sigma(F)$] = 0.0820.

Polymorph	α	α	α	β	γ	γ	γ	δ	ε
Pressure (GPa)	Ambient	2.0	6.2	Ambient	Ambient	0.5	1.3	1.9	4.3
Crystal System	Monoclinic	Monoclinic	Monoclinic	Monoclinic	Trigonal	Trigonal	Trigonal	Monoclinic	Monoclinic
Space group	$P2_1/n$	$P2_1/n$	$P2_1/n$	$P2_1$	$P3_1$	$P3_1$	$P3_1$	$P2_1/a$	Pn
a/Å	5.1047(3)	4.9669(9)	4.8690(7)	5.0932(16)	7.0383(7)	6.9332(6)	6.8617(4)	11.156(4)	4.8887(10)
b/Å	11.9720(14)	11.459(4)	11.139(3)	6.272(3)	= a	= a	= a	5.8644(11)	5.7541(11)
c/Å	5.4631(3)	5.4231(12)	5.3777(10)	5.3852(18)	5.4813(8)	5.4552(8)	5.4282(6)	5.3417(17)	5.4419(11)
β/°	111.740(5)	114.916(15)	116.888(11)	113.19(3)	= 90	= 90	= 90	125.83(4)	116.682(10)
V/Å^3	310.10(4)	279.92(13)	260.14(10)	158.13(9)	235.15(3)	227.10(4)	221.33(3)	283.32(16)	136.78(5)
Z	4	4	4	2	3	3	3	4	2
$R_1[F>4\sigma(F)]$	*Ref 18*	0.0771	0.0685	*Ref 18*	*Ref 18*	0.0866	0.0895	0.0759	$R_{wp=}$ 0.0135
θ_{max}/°	*Ref 18*	22.4	24.3	*Ref 18*	*Ref 18*	23.1	23.1	23.2	12.0 λ = 0.4654 Å
Observations	*Ref 18*	128	149	*Ref 18*	*Ref 18*	134	125	199	-
Restraints	*Ref 18*	8	8	*Ref 18*	*Ref 18*	9	9	8	-
Parameters	*Ref 18*	22	21	*Ref 18*	*Ref 18*	22	22	21	34

Table 1. Crystallographic data for α, β, γ, δ (obtained by compression of the β-phase) and ε-glycine (from the γ-phase). Ambient pressure data for α, β and γ glycine are taken from ref. 18 (CSD refcodes GLYGLY29, GLYGLY31 and GLYGLY33, respectively). High pressure structures were determined as part of this study. All crystals were colorless blocks with molecular formula $C_2H_5NO_2$ and formula weight 75.07. Full listings of crystallographic data are available in *cif* format in the supplemental material. All refinements were carried out against F^2 using all data; the values of R_1 quoted below were calculated on F using data with $F > 4\sigma(F)$. 1.0 GPa = 10 kbar. All data were collected at room temperature.

The problem of crystal movement, though still present, was much less severe at 1.9 GPa, possibly as a result of increased viscosity in the hydrostatic medium. It is therefore these results that are reported here. The structure of the new phase was solved by direct methods[57] and refined as described above. The orientation of the NH_3^+ group was established by location of one H-atom in a difference Fourier map. The final conventional R factor [calculated on $|F|$ and 149 data with $|F| > 4\sigma(|F|)$] for the refinement against the 1.9 GPa data set was 0.0759. Some data collection and refinement statistics are given in Table 1, the remainder are available in the

cifs that form the supplemental data to this paper. The structure of δ-glycine is described here in its $P2_1/a$ setting; this was chosen in order to facilitate comparisons with the other polymorphs described here.

After collection of the data-set at 1.9 GPa the pressure was released, and the sample recovered from the diamond anvil cell. The phase on return to ambient pressure was identified as β-glycine on the basis of its unit cell dimensions [monoclinic, a = 5.083(8), b = 6.270(10), c = 5.380(9) Å, β = 113.09(2)°].

The compression of γ-glycine studied by single crystal X-ray diffraction

A single crystal of γ-glycine was loaded into a Merrill-Bassett pressure cell and a data set collected at ambient pressure to establish the starting phase, and then at 0.5, 1.3 and 1.9 GPa. The ambient pressure cell dimensions were found to be trigonal, a = 7.0362(3), c = 5.4771(5) Å (*cf* Table 1). Though a data set collected at 1.3 GPa suffered from peak-broadening (Figure 2), sufficient data were collected to enable refinement of the structure at this pressure. By 1.9 GPa, however, the peaks were too broad to yield useful single crystal data, and it appeared that a phase transition was occurring to a polycrystalline material. This transformation was later identified as the γ-to-δ transition in a separate powder diffraction study (see below). The sample was found to be merohedrally twinned *via* a two-fold axis along [110]; the twin law matrix was

$$\begin{pmatrix} 0 & 1 & 0 \\ 1 & 0 & 0 \\ 0 & 0 & -1 \end{pmatrix},$$

and the twin scale factors refined to 0.22(2) and 0.19(2) at 0.5 and 1.3 GPa, respectively. Data collection and refinement statistics for γ-glycine at 0.5 and 1.3 GPa are presented in Table 1.

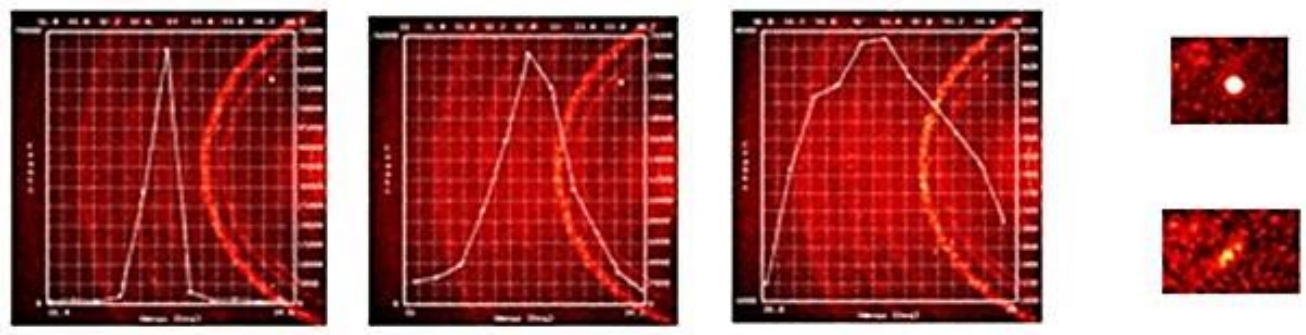

Figure 2. Broadening of the diffraction profiles of γ-glycine with pressure. Frames taken at (*a*) 0.5, (*b*) 1.3 and (*c*)1.9 GPa. (*d*) Close-up of one diffraction peak at 0.5 and 1.9 GPa.

The compression of γ-glycine studied by synchrotron powder diffraction

A polycrystalline sample of the γ-glycine was obtained by crushing a single crystal of γ-glycine (previously identified from its cell dimensions, as determined by single crystal methods). Paraffin was used as the pressure-transmitting medium. Data collections were carried out at Station 9.1 at the SRS, Daresbury, using the experimental procedures described by Nelmes and McMahon.[58] The wavelength used was 0.4654 Å. Debye-Scherrer rings were recorded on an image plate, and integrated using the program EDIPUS.[59] Data were recorded at ambient pressure and at 4.3 GPa. The pressure was then released and two further data-sets recorded, one immediately following pressure release and the second after eight hours.

Two high pressure phases of glycine have been structurally characterized: the δ-phase described here and the ε-phase identified by Boldyreva.[32] Rietveld refinement for each powder pattern was carried out using TOPAS-A.[60,61] Initial cell dimensions and atomic coordinates for the γ and ε-phases were taken from refs 18 and 32. We have changed the atom-labelling and unit cell setting from that used in ref. 32 of ε-glycine to be consistent with those of the other polymorphs described here using the matrix:

$$\begin{pmatrix} 0 & 0 & 1 \\ 0 & -1 & 0 \\ 1 & 0 & 0 \end{pmatrix}.$$

The glycine zwitterions were modelled as rigid bodies using the Z-matrix formalism available in TOPAS. The background was modelled using a six-term Chebychev polynomial. Preferred orientation effects were modelled using fourth-order spherical harmonic expansions[62] for ε glycine, and the March-Dollase method[63] in the [0 0 1] direction for γ-glycine.[31] The powder pattern at ambient pressure (Figure 3*a*) could be modelled as 100% γ-glycine; final refinement statistics are given in the caption to Figure 3.

A Pawley-fit[64] of a model consisting of six background terms, the unit cell dimensions and Lorenzian and Gaussian strain parameters against the data obtained at 4.3 GPa yielded R_{wp} = 1.35%.

A model consisting of a mixture of δ and γ glycine was refined against these data to yield R_{wp} = 2.59% (Figure 3*b*).

Rietveld refinement of Boldyreva's structural model of ε-glycine obtained at 7.85 GPa yielded R_{wp} = 2.73%. We have obtained a rather better fit by re-optimising the orientation of the molecule in the unit cell using simulated annealing,[65] while retaining Boldyreva's position, space group and indexing. Refinement of the new model yielded R_{wp} = 1.56%, and this reduced to 1.35% when a small amount of γ-glycine was also included in the model. A plot of the pattern is shown in Figure 3*c*.

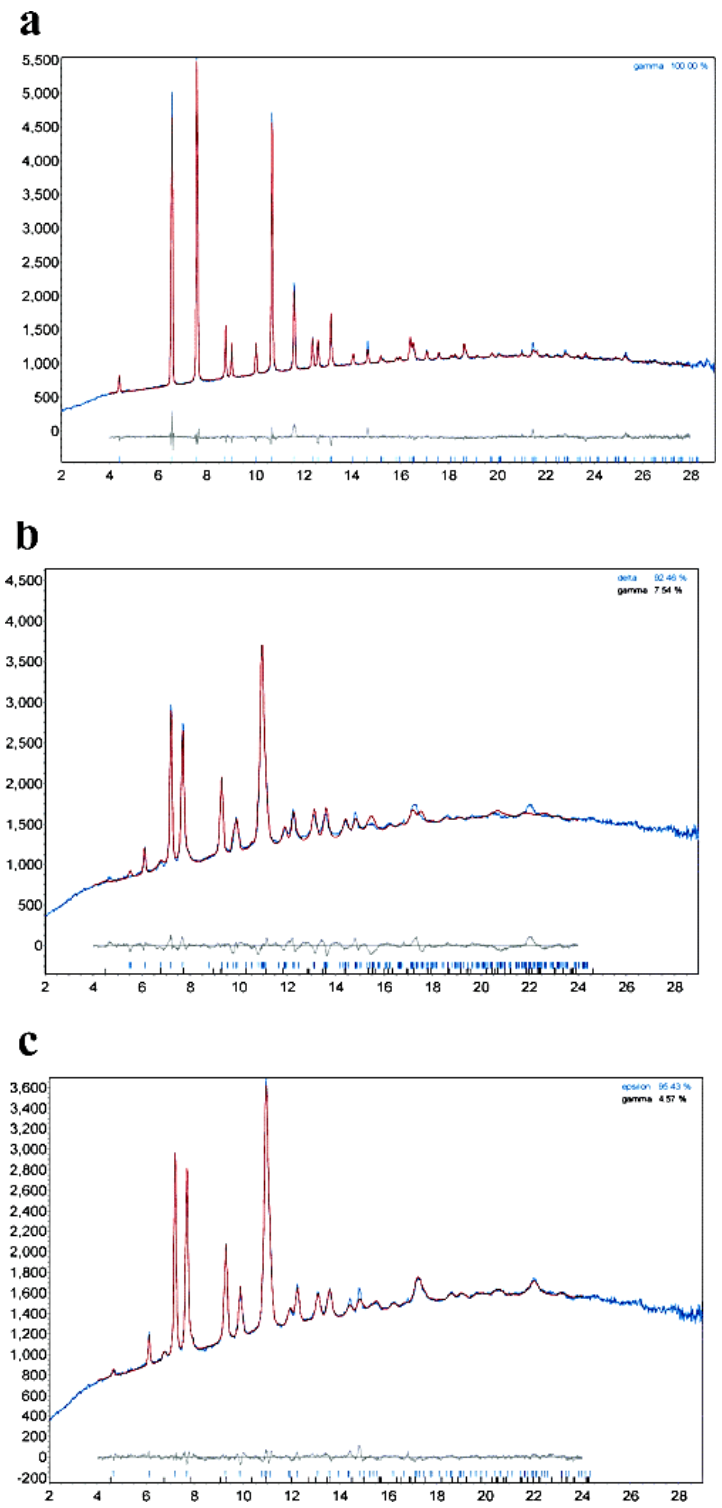

← ***Figure 3.*** Compression of γ-glycine as studied by synchrotron powder diffraction. (*a*) Sample at zero pressure modelled using γ-glycine coordinates. Refined cell dimensions: a = 7.0354(3), c = 5.4791(2) Å, V = 234.86(2) Å^3. R_{wp} = 2.21%. (*b*) Pattern at 4.3 GPa fitted to a mixture of γ and δ-glycine. The refined cell dimensions for γ-glycine are a = 6.892(8), c = 5.228(15) Å, V = 215.10(8) Å^3. Those for δ-glycine are a =10.833(3), b = 5.7429(15), c = 5.431(2) Å, β = 126.503(16)°, V = 271.58(16) Å^3. The refined proportion of the δ-phase is 92.5(7)%. R_{wp} is 2.46%. (*c*) Pattern at 4.3 GPa fitted to a mixture of γ and ε-glycine. The refined cell dimensions for γ-glycine are a = 6.804(6), c = 5.358(9) Å, V = 214.8(5) Å^3. Those for ε-glycine are a = 4.8887(10), b = 5.7542(11), c = 5.4419(11) Å, β = 116.682(10) °, V = 136.78(5) Å^3. The corresponding values obtained at 7.85 GPa by Boldyreva (but with a different structural model) are a = 4.780(1), b = 5.557(1), c = 5.379(1) Å, β = 118.25(1)Å, V = 125.86(1) Å^3. The refined proportion of the δ-phase is 95.4(4)%. R_{wp} is 1.35%.

Results and Discussion

Compression Study of α-Glycine

α-Glycine crystallizes in space group $P2_1/n$ with one molecule in the asymmetric unit. It is the polymorph of glycine most commonly obtained by recrystallisation from aqueous solution. It was long thought that this

implies that it is the most stable polymorph, though it is now recognized that the γ-glycine is slightly more stable under ambient conditions.[19,20] The glycine molecules are present as the zwitterionic tautomer (Scheme 1), as is the case in all polymorphs described here.

The crystal structures of all phases of glycine are built-up of chains of glycine molecules interacting *via* N1-H3…O2 H-bonds (see Table 2 for dimensions and symmetry operators and Figure 4*a*);[15,20,26] these chains have the primary graph-set descriptor $C(5)$,[66] and they define lattice-repeats along the *c*-axis directions of all polymorphs described here. Somewhat longer H-bonds, involving the atoms N1-H4…O1, are formed between the chains to build up a layer which sits parallel to the *ac* plane (Figure 4*b* and *c*). This second set of H-bonds also builds-up $C(5)$ chains, and these run along the *a*-axis direction. At the secondary level these two sets of $C(5)$ chains form $R_4^4(16)$ ring motifs.

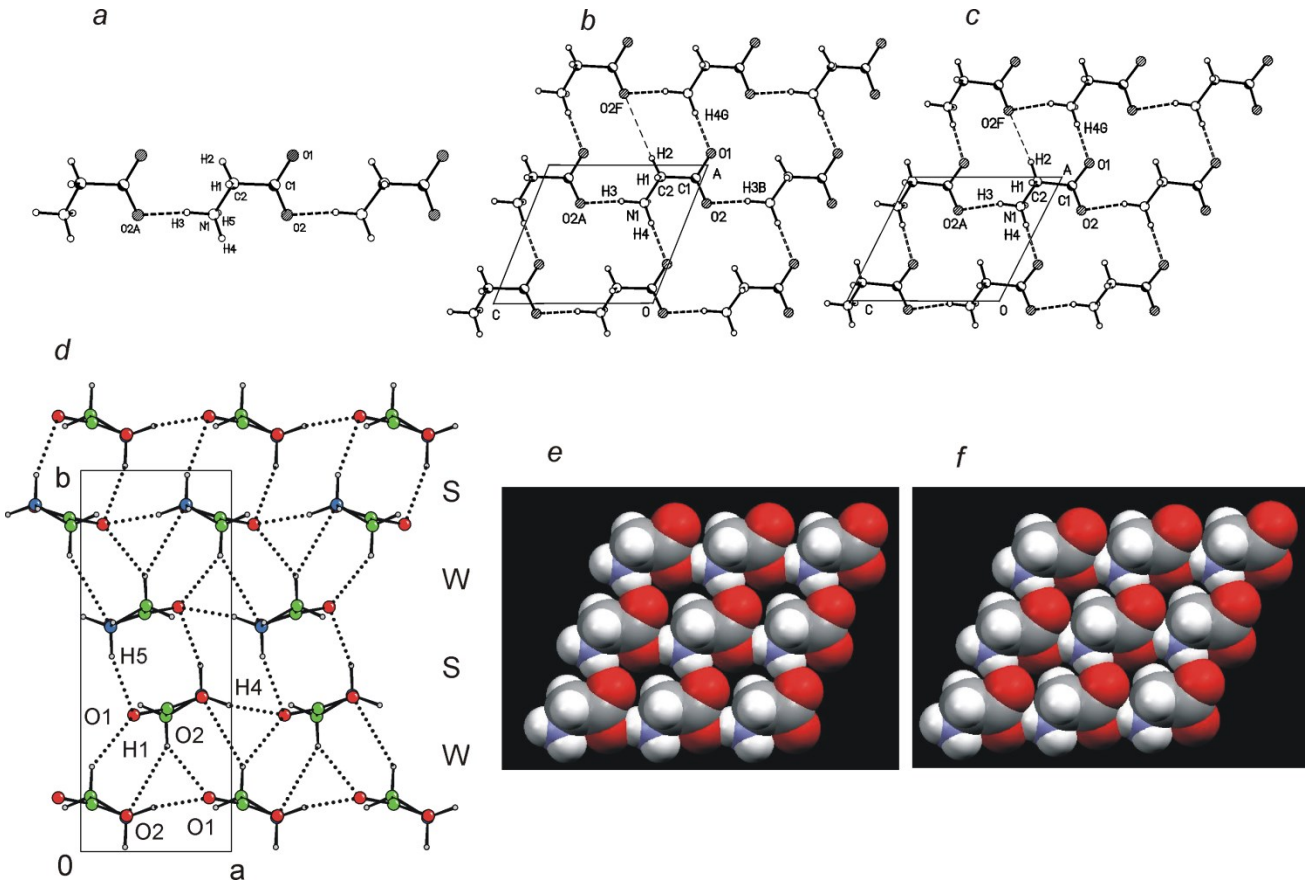

Figure 4. The crystal structure of α-glycine. (*a*) $C(5)$ chains linked by NH…O hydrogen bonds run along the *c*-axis of all the polymorphs described in this paper. (*b*) and (*c*) Views of the layers of molecules formed parallel to the *ac* planes at ambient pressure and 6.2 GPa, respectively. The hydrogen bonds in the $C(5)$ chains shown in part (*a*) are shown as shaded dotted lines, those forming the $C(5)$ chains which run along *a* are shown in open dashed lines. One trans-annular CH…O interaction, which bridges across an $R_4^4(16)$ ring, is shown in each case; this distance is 3.05 Å at ambient pressure and 2.50 Å at 6.2 GPa. (*d*) Stacking of the layers along the *b*-direction. Regions of short NH…O hydrogen bonds and weak CH…O hydrogen bonds are

indicated with the letters ‘S’ and ‘W’. (*e*) and (*f*) Space-filling representations of (*b*) and (*c*) showing the closing up of the voids in the middle of the $R_4^4(16)$ rings with application of pressure.

α-Glycine	0 GPa			6.2 GPa		
τ(O2C1C2N1)/°	-19.01(10)			-11.6(16)		
Contacts:	N/C…O /Å	H…O /Å	<N/CHO /°	N/C…O /Å	H…O /Å	<N/CHO /°
N1H3…O2(i)	2.7703(9)	1.788(17)	167.2(15)	2.740(7)	1.90	157
N1H4…O1(ii)	2.8507(10)	1.899(16)	170.0(11)	2.721(9)	1.83	173
N1H5…O1(iii)	3.0748(11)	2.183(15)	156.4(17)	3.031(18)	2.18	160
C2H1…O1(iv)	3.2739(11)	2.488(15)	139.9(13)	2.968(14)	2.25	130
C2H1…O2(v)	3.3593(11)	2.559(13)	142.0(13)	3.117(17)	2.28	144
C2H2…O2(iii)	3.4098(11)	2.859(13)	118.0(10)	3.051(15)	2.55	112
C2H2…O2(vi)	3.9742(11)	3.054(16)	163.3(10)	3.449(8)	2.50	167
β and δ Glycine	β Glycine at 0 GPa			δ-Glycine at 1.9 GPa		
τ(O2C1C2N1)/°	25.03(12)			-27.7(8)		
Contacts:	N/C…O /Å	H…O /Å	<N/CHO /°	N/C…O /Å	H…O /Å	<N/CHO /°
N1H3…O2(i)	2.7628(16)	1.864(17)	174.4(16)	2.762(10)	1.92	157
N1H4…O1(ii)	2.8506(17)	1.97(2)	177(2)	2.782(13)	2.01	144
N1H5…O1(iii)	2.9780(18)	2.23	140.8(18)	2.876(7)	2.17	136
N1H5…O2(iv)	2.9787(19)	2.30(2)	132.4(18)	2.916(8)	2.21	136
C2H1…O1(v)	3.322(2)	2.56(2)	138.3(16)	3.159(7)	2.39	135
C2H1…O2(vi)	3.923(2)	3.19(2)	135.9(16)	3.247(8)	2.51	132
C2H2…O2(vii)	3.706(2)	2.82(2)	152.8(15)	3.495(13)	2.56	161
γ-Glycine	0 GPa			1.3 GPa		
τ(O2C1C2N1)/°	15.4(4)			15(3)		
Contacts:	N/C…O /Å	H…O /Å	<N/CHO /°	N/C…O /Å	H…O /Å	<N/CHO /°
N1H3…O2(i)	2.804(3)	1.93	168	2.766(12)	1.90	166
N1H4…O1(ii)	2.811(5)	1.98	154	2.78(3)	1.97	151
N1H5…O2(iii)	2.976(5)	2.11	166	2.89(3)	2.02	165
O2…O2(iv)	O…O = 3.319(4)	-	-	O…O = 3.219(18)	-	-

Symmetry codes:

α-Glycine: (i) *x*, *y*, *z*+1; (ii) *x*-1, *y*, *z*; (iii) 2-*x*, 2-*y*, -*z*; (iv) -1/2+*x*, 3/2-*y*, 1/2+*z*; (v)1/2+*x*, 3/2-*y*, 1/2+*z*; (vi) 1+*x*, *y*, 1+*z*

β-Glycine: (i) *x*, *y*, -1+*z*; (ii) 1+*x*, *y*, *z*; (iii) –*x*, -1/2+*y*, 1-*z*; (iv) 1-*x*, -1/2+*y*, 1-*z*; (v) –*x*, 1/2+*y*, 1-*z*; (vi) 1-*x*, 1/2+*y*, 1-*z*; (vii) 1-*x*, *y*, -1+*z*

δ-Glycine: (i) *x*, *y*, 1+*z*; (ii) 1/2+*x*, 3/2-*y*, 1+*z* ; (iii) 3/2-*x*, -1/2+*y*, 2-*z*; (iv) 2-*x*, 1-*y*, 3-*z*; (v) 3/2-*x*, 1/2+*y*, 2-*z*; (vi) 2-*x*, 2-*y*, 3-*z*; (vii) -1/2+*x*, 3/2-*y*, *z*.

γ-Glycine: (i) *x*, *y*, -1+*z*; (ii) 1-*x*+*y*, 1-*x*, -1/3+*z*; (iii) 2-*x*+*y*, 1-*x*, -1/3+*z*; (vi) 1-*y*, -1+*x*-*y*, 1/3+*z*.

Table 2. Hydrogen bond and contact distances and angles in α, β, γ and δ-glycine. Standard uncertainties are only quoted where the atoms involved were refined. Distances involving H are derived from the X-ray results directly, and have not been normalized to typical neutron values.

The layers are stacked along the *b*-direction. Pairs of H-bonds, related by crystallographic inversion centers, are formed between N1-H5…O1 in $R_2^2(10)$ (primary level) motifs.[67] The effect of this is to build up a bi-layer (or double-layer) structure in which pairs of layers are H-bonded together, with the bi-layers interacting with each other *via* longer three-center C1-H1…O1 and C1-H1…O2 interactions, in which H1 bridges neighbouring glycine molecules in the *C*(5) chains running along the *a*-axis (Figure 4*d*).

Application of high hydrostatic pressure shortens the three unit cell dimensions of α-glycine (Table 1). The effect is anisotropic, and between ambient pressure and 6.2 GPa the unit cell *c* dimension changes least (-1.6%) and the *b*-axis the most (-7.0%), with the *a*-axis changing by -4.6%; the β-angle increases from 111.740(5)° to 116.888(11)°. These results are consistent with those obtained by Boldyreva in a powder study of a mixture of α and γ glycine up to 4.0 GPa.[31] Intramolecular bond distances and angles were restrained to be equal to those observed at ambient pressure; removal of the restraints did not lead to significantly different values for the bond lengths and angles, though their standard uncertainties were some 50% higher. The only distortion in the molecular dimensions on application of pressure is a reduction in the N1-C2-C1-O2 torsion angle, which is -19.01(10)° at ambient pressure and -11.6(16)° at 6.2 GPa. Note that the signs of the torsion angles are not important: the space group symmetry generates other molecules with positive torsion angles.

The changes in *a*, *c* and β reflect the effect of pressure on the structure of the layers in the crystal structure of α-glycine. The variation of the *b*-axis length reflects the way in which the stacking of the layers changes, and it is clear that one effect of high pressure is to reduce the stacking distance between the layers. The H-bonds between N1-H5…O1, which form the bi-layers, do not change much on application of pressure [N1…O1 = 3.0748(11) Å at ambient pressure and 3.031(18) Å at 6.2 GPa; the H…O distance is 2.18 Å at both pressures, though it should be stressed that H-atom positions were idealized to typical X-ray values during refinement]. By contrast, the softer C2H2…O2 interactions between these bilayers shorten significantly, from 2.84 Å at ambient pressure to 2.55 Å at 6.2 GPa. The reduction in the CH…O hydrogen-bond lengths between the bi-layers is also notable: the bifurcated C1-H1…O1/2 distances are 2.49 and 2.56 Å at ambient pressure and 2.25 and 2.28 Å at 6.2 GPa. These distances are derived from X-ray measurements, which tend to place H-atoms too close to their directly-bonded atoms. 'Normalisation' of the C-H bonds to typical values observed in neutron diffraction reduces these distances to 2.17 and 2.19 Å, respectively, values near to the minimum observed for such interactions at ambient pressure.[68]

The separation of the bilayers (*i.e.* layers connected by NH…O interactions) is reduced by 0.109 Å from 0 to 6.2 GPa; the effect of pressure on the layers connected by only CH…O interactions is almost three times greater (0.307 Å). In the *b*-direction the effect of pressure is therefore largely to reduce the CH…O distances between the layers. Compression of the layers is presumably the reason that the magnitude of the O2-C1-C2-N1 torsion angle decreases slightly with increasing pressure as this reduces the height of the molecules measured in the *b*-axis direction.

In low-symmetry crystal systems straightforward examination of the variation of the unit-cell dimensions with pressure (or temperature) may not reveal the most significant structural changes, and calculation of the eigenvalues and eigenvectors of the strain ellipsoid is necessary.[52a] In a monoclinic crystal one principal direction of the strain ellipsoid must lie along the *b*-direction, but although the *b*-axis showed the greatest relative shortening on application of pressure, this is not the direction of greatest linear strain.

The largest eigenvalue of the strain ellipsoid (calculated by comparing unit cell dimensions at 0 and 6.2 GPa) lies with its eigenvector within the layers, *i.e.* in the *ac* plane, making angles of 45° and 67° with the *a* and *c* axes, respectively. A space-filling plot of the structure of α-glycine at ambient pressure is shown in Figure 4*e*; the 'holes' in the layers correspond to the centers of the $R_4^4(16)$ ring motifs. The principal strain eigenvector is almost parallel (angle 4.8°) to the trans-annular C2H2…O2 vector formed across the $R_4^4(16)$ rings, in which the H2…O2 distance decreases from 3.05 Å at ambient pressure to 2.50 Å at 6.2 GPa (this vector is indicated by a dashed line in Figure 4*b*. It is also approximately perpendicular (angle: 87.5°) to the C1-N1 axis of the glycine molecules. Figure 4*f* shows a space filling plot of α-glycine at 6.2 GPa, and, by comparison with Figure 4*e*, it is evident that the consequence of compression is a more efficiently space-filling packing in the layers, with the molecules adopting a more close-packed arrangement. Once again, this is also associated with the formation of a CH…O interaction.

Our description of the effect of pressure on α-glycine has so-far focussed on the strengthening of weak CH…O hydrogen bonds, but how does pressure affect the stronger NH…O interactions? The principal strain eigenvector lies almost parallel (angle: 9.7°) to the N1-H4…O1 H-bond, and one effect of compression is to reduce the length of this interaction from N1…O1 = 2.8507(10) Å at ambient pressure to 2.721(9) Å at 6.2 GPa. This hydrogen bond is also approximately parallel to the CH…O interaction which forms across the $R_4^4(16)$ rings, and its shortening may be associated with formation of the weak hydrogen bond and the closing-up of the holes in the middle of this rings. The change is less in N1-H3…O2, the other, stronger, *C*(5)-forming H-bond which builds-up the *ac* layers: the N1…O2 distance in this interaction is 2.7703(9) Å at ambient pressure and 2.740(7) Å at 6.2 GPa. In fact the H3…O2 distance actually appears to increase at 6.2 GPa (1.90 Å) relative to that at ambient pressure (1.79 Å), while the angle subtended at the calculated H3 site decreases from 167.2(15)° to 157° in passing from ambient pressure to 6.2 GPa. It is apparent that H3 begins to bifurcate more strongly between the oxygen atoms of the carboxylate group involved in this interaction, with N1…O1 being reduced from 3.428(10) Å at ambient pressure to 3.120(8) Å at 6.2 GPa.[35] Similar effects have been observed in L-serine.[9] These effects are also arguably driven by the 'closing-up' of the $R_4^4(16)$ rings.

The smallest strain component is not significantly different from zero [+0.00025(12)], and its eigenvector makes a small angle (20.4°) with the N1-H3…O2. This is consistent with the expectation that the strongest intermolecular interaction should correspond, at least approximately, to the direction of smallest compression.

The Structural Relationship Between α and β-Glycine

The crystal structure of β-glycine is quite similar to that of the α-polymorph, though the β-form is the less stable, and will undergo conversion to the α-form under humid conditions. The structure of β-glycine was only determined in this study for the purposes of phase identification, and our motive for discussing it here is to highlight its structural relationship with the other polymorphs. The data quoted are taken from Boldyreva's room-temperature structure (CSD refcode GLYCIN31).[18]

The strongest interaction between the molecules is a *C*(5) chain-building N1-H3…O2 hydrogen bond. This chain is built by lattice repeats along **c**. The next-strongest hydrogen bonds, which link the chains together into a layer, are formed between N1-H4…O1, also building-up *C*(5) chains in which neighbouring molecules are related by lattice repeats along **a**. The intersection of these two sets of *C*(5) chains creates $R_4^4(16)$ rings at the second level of graph set analysis (Figure 5*a*). The structure of the layers is therefore identical to that in the α-polymorph. Comparison of Figures 4*e* and 5*a* shows that packing in the layers in β-glycine is more efficient than in α-glycine: there are smaller holes in the middle of the $R_4^4(16)$ rings (the H2…O2 distances in α and β-glycine are 3.05 and 2.81 Å, respectively), while the area of the *ac*-face is smaller in the β form (25.9 $Å^2$ *versus* 25.2 $Å^2$ for α and β, respectively)

The H-bonded layers are regularly stacked along the *b*-axis, being related by 2_1 operations (Figure 5*b*). A three-center hydrogen bond is formed from N1-H5 to O1 and O2 in the layer below, the oxygen atoms being neighbours in a *C*(5) chain running along **a**. A secondary C2-H1…O1 hydrogen bond (H…O = 2.56 Å) also links the layers together. In α-glycine a similar inter-layer interaction was bifurcated; it is not so here: the next shortest interaction from H1 is to O2, and measures 3.19 Å. All layers are therefore linked by NH…O hydrogen bonds (this contrasts with the bilayer structure of α-glycine, see above). The structure is polar: in Figure 5*b* all the molecules are oriented so that H5 points down. The interlayer separation is 3.136 Å, and this is larger than the mean layer-separation in α-glycine (2.993 Å). Although the packing within the layers in more efficient in the β-glycine, the stacking of the layers is more efficient in the α-polymorph, which has the greater density (1.608 Mg m^{-3} versus 1.577 Mg m^{-3}, both values at ambient pressure), and higher stability.

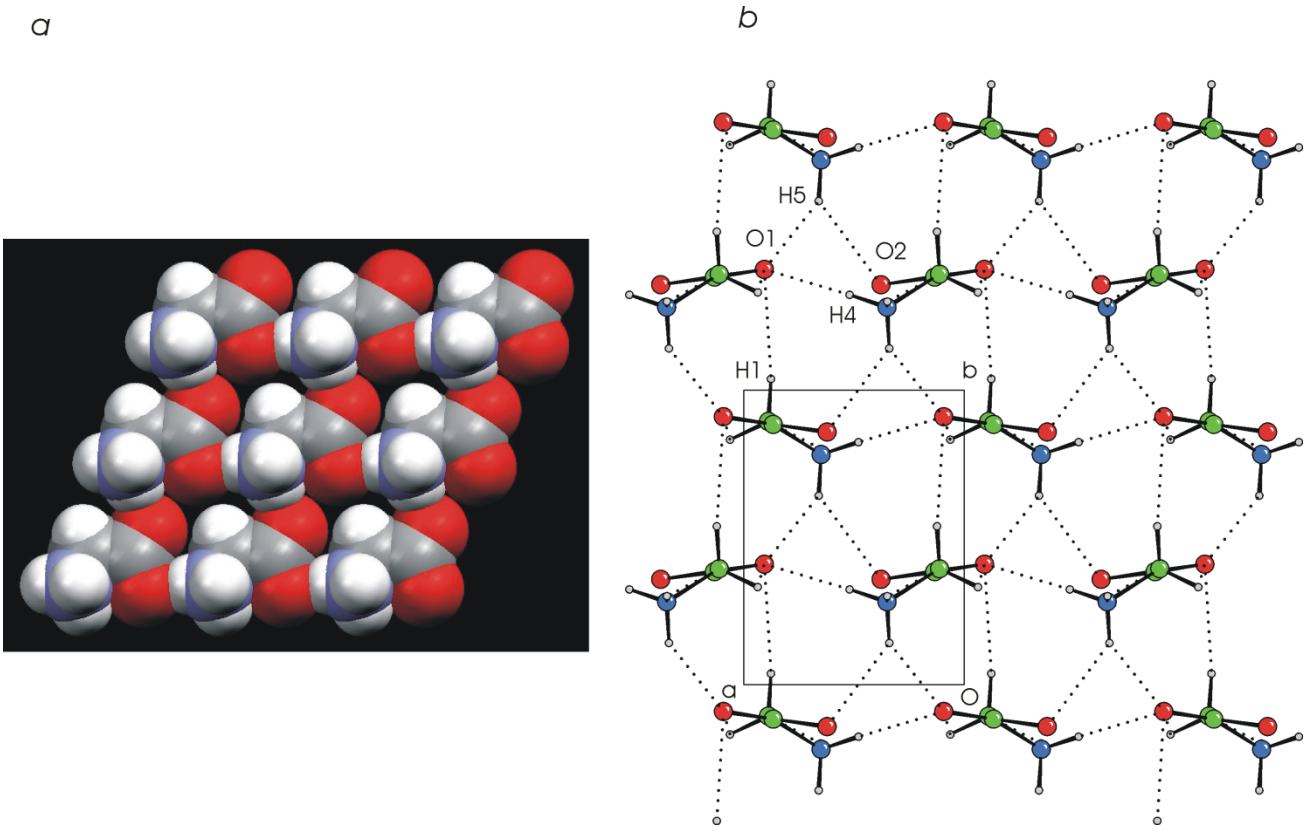

Figure 5. The crystal structure of β-glycine at ambient pressure. (*a*) Space filling plot of a hydrogen-bonded layer formed parallel to the *ac* face. (*b*) NH…O and CH…O interactions between layers stacked along the *b*-direction.

δ-Glycine

Although the crystal structures of α and β glycine are similar, their responses to hydrostatic pressure are quite different. Raman spectroscopy measurements indicate that α-glycine persists to at least 23 GPa. By contrast, β-glycine undergoes a reversible single-crystal to single-crystal phase transition at 0.8 GPa to δ-glycine. The same phase transition was also recently detected at 0.76 GPa by Boldyreva using Raman spectroscopy.[10b]

As in the structures of α and β-glycine, the strongest hydrogen bonds in δ-glycine form a *C*(5) chain motif by lattice repeats along **c** (Figure 6*a*). A second *C*(5) chain forms along **a** through N1H4…O1 hydrogen bonds. Successive molecules in this second chain are related by the *a*-glide, not the *a* lattice repeat, and for this reason the *a*-cell dimension is approximately double those observed in α and β-glycine. The molecules occupy the *a*-glide planes at y = ¼ and ¾, and so this arrangement still builds-up layers perpendicular to the *b*-axis, but rather than all molecules in one layer being in the same orientation, half of them are reflected in the *ac* plane. The areas of the *ac* planes in α-glycine at 2.0 GPa, β-glycine at ambient pressure and δ-glycine at 1.9 GPa are 24.42, 25.21 and 24.15 Å^2 molecule^{-1}, showing that the arrangement within the layers in δ-glycine

is more efficiently space-filling than in the other polymorphs. The combination of the two $C(5)$ chains creates $R^4_4(16)$ rings (Figure 6*a*), and, comparison with Figure 5*a*, reveals that one effect of the β-to-δ phase transition has been to close-up the voids in the middle of the rings. This is similar to the effect observed in α-glycine, and it also acts to form a trans-annular C2H2…O2 interaction (2.56 Å, *cf.* 2.82 Å in β-glycine at ambient pressure and 2.71 Å in α-glycine at 2.0 GPa).

Successive molecules in each layer form three-center N1-H5…O1/2 hydrogen bonds to the layers above and below (Figure 6*b*). This arrangement contrasts to β-glycine, where the sense of the donor-to-acceptor interaction is unidirectional (H5 always points down in Figure 5*b*), but there is a clear relationship between the distributions of interlayer hydrogen bonds in the two polymorphs and the introduction of the *a*-glide plane in the δ-polymorph. There is an additional, bifurcated, C2H1…O1/2 hydrogen bond (H…O = 2.39 and 2.51 Å) also formed between the layers. This interaction is the result of the bifurcation of the inter-layer C2H1…O1/2 hydrogen bond (2.56 and 3.19 Å) of β-glycine. The interlayer separation in δ-glycine is 2.932 Å. This compares to 3.136 Å in β-glycine at ambient pressure and an average of 2.865 Å in α-glycine at 2.0 GPa. Under similar conditions of pressure (1.9 and 2.0 GPa), therefore, the layers in α-glycine are more efficiently stacked than in δ-glycine, and as a result the density of α-glycine (1.781 Mg m^{-3}) is higher than that of δ-glycine (1.760 Mg m^{-3}).

The O2-C1-C2-N1 torsion angle in β-glycine is 25.03(12)°; since, loosely speaking, $P2_1$ is a chiral space group, all torsion angles within the same single crystal have the same sign. In δ-glycine, which is centrosymmetric, there are equal numbers of molecules with positive and negative torsion angles [±27.7(8)°]. It is known from molecular modelling studies that torsion angles are quite 'soft' parameters, and the development of δ-glycine from β-glycine can be viewed as a concerted inversion of the O1-C1-C2-N1 torsion angles in alternate molecules. This change does not involve changes in the orientation or relative positions of the glycine molecules, and this is consistent with the β-to-δ being reversible and non-destructive.

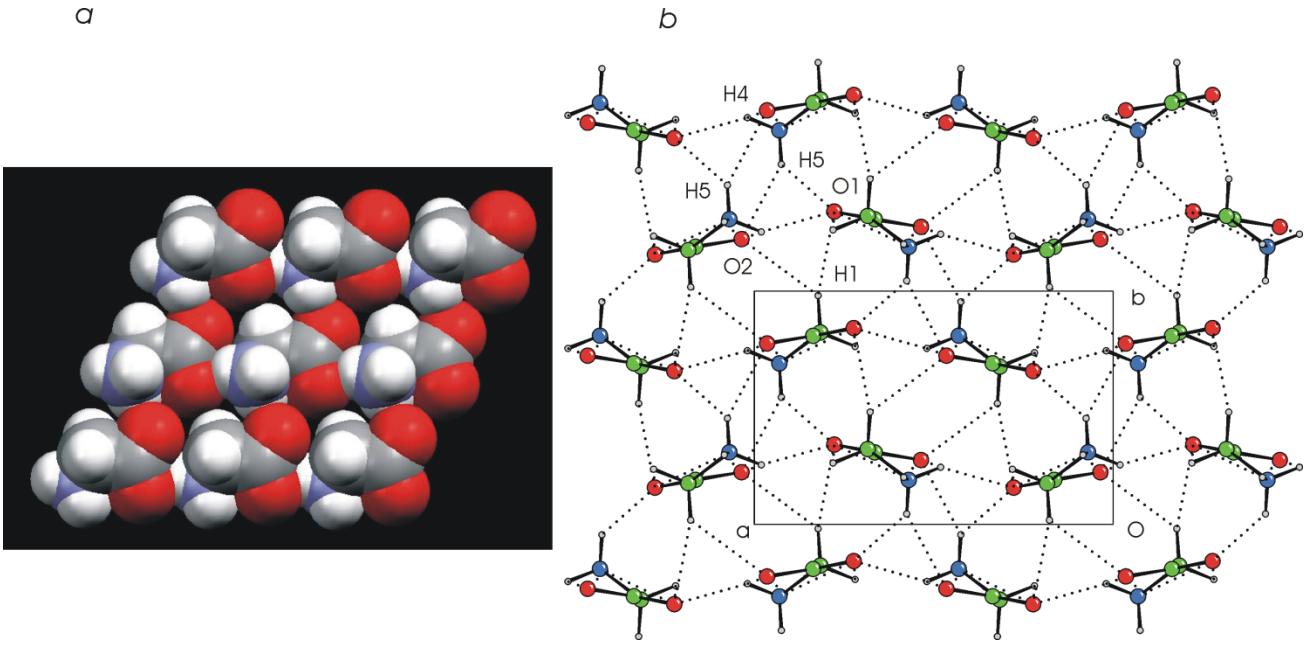

Figure 6. Hydrogen bonded layers (*a*) and layer stacking (*b*) in the crystal structure of δ-glycine at 1.9 GPa. This figure should be compared to Figure 5: note the more efficient packing in 6*a* compared to 5*a*, and the greater number of CH…O hydrogen bonds between the layers in 6*b*.

The Effect of Pressure on γ-Glycine.

γ-Glycine is trigonal, crystallizing in the chiral space groups $P3_1$ and $P3_2$. Its crystal structure (available as CSD refcode GLYCIN33)[18] does not consist of layers, but is a three-dimensional hydrogen-bonded network. Molecules form helices around the 3_1 screw-axis at 0,0,*z*, successive molecules being linked by N1-H5…O2 hydrogen bonds; Figure 7*a* shows the structure projected onto (001) with different helices color-coded. Hydrogen bonds between N1-H3…O2 are formed between each molecule and its symmetry equivalent three molecules away along the helix, *i.e.* related by one lattice repeat along **c** (Figure 7*b*). Taken on their own these N1-H3…O2 H-bonds form the same *C*(5) chain as was observed along the *c* directions of the other polymorphs. The helices are linked together by N1-H4…O2 hydrogen bonds which lie around other 3_1 screw axes. The hydrogen bond most affected by pressure is N1-H5…O2, and this is associated with the closing-up of non-bonded O2…O2 distances within the helices centred at 0,0,*z* from 3.319 Å at ambient pressure to 3.219 Å at 1.3 GPa (Figure 7*c*). The N1-H4…O1 and N1-H3…O2 hydrogen bond geometries are very similar at ambient pressure and 1.3 GPa. CH…O interactions seem to be of less significance in the structure of γ-glycine than in those of the other polymorphs: C2H2…O1(2-*y*, *x*-*y*, -2/3+*z*), which is 2.64 Å at ambient pressure and 2.61 Å at 1.3 GPa, is the only such interaction measuring less than the sum of the van der Waals radii of H and O (though this criterion is criticised in reference34*b*). Boldyreva has suggested on the basis of changes in the cell dimensions of γ-glycine that conformational adjustments of the glycine molecules take place on

application of pressure.[31] This is consistent with our results on α and β glycine, but our data on γ-glycine are of insufficient precision to detect similar changes in the N1-C2-C1-O2 torsion angle.

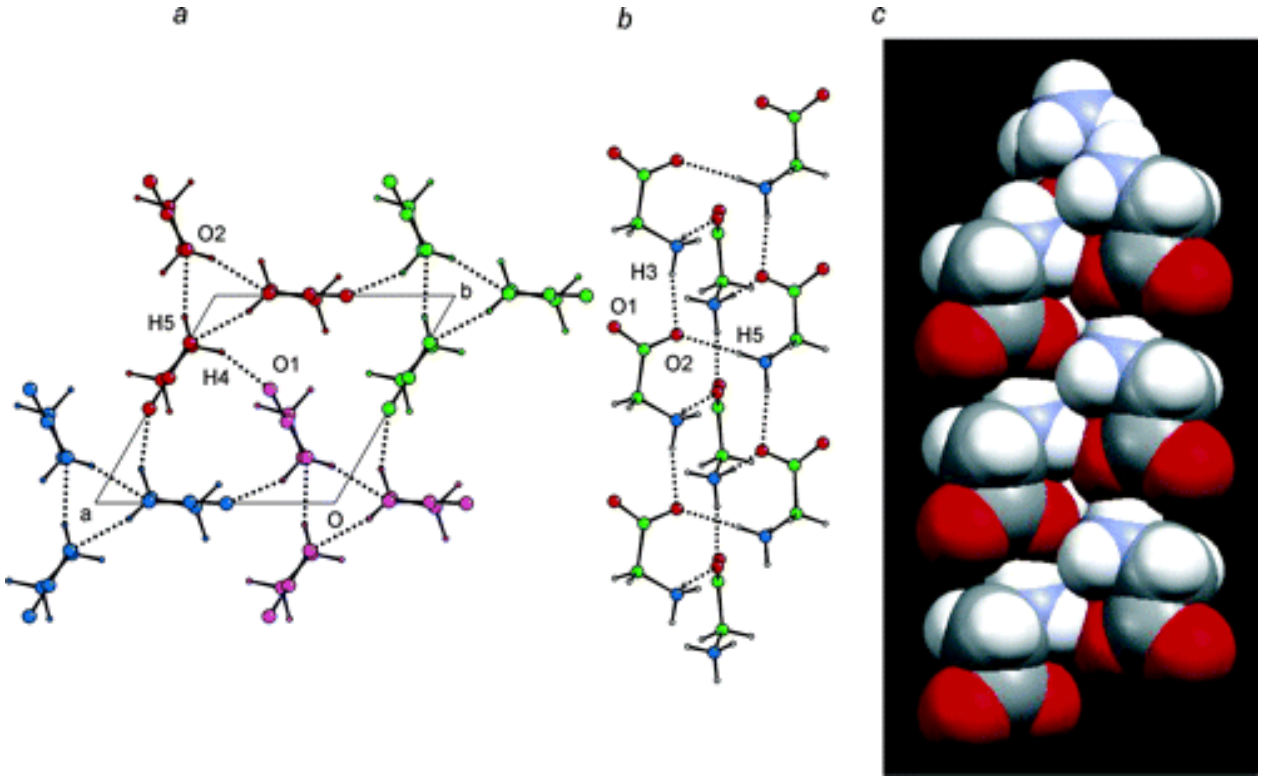

Figure 7. The crystal structure of γ-glycine at 1.3 GPa. (*a*) Molecules form helices about 3_1 axes passing through the origin (0, 0, *z*); each helix is shown in a different color. These helices are linked together about other 3_1 axes. (*b*) One of the helices passing through (0, 0, *z*). Taken on their own the chains formed by the H3…O2 interactions form a similar motif to that shown in Figure 4*a*. (*c*) Application of pressure decreases non-bonded O…O distances within the helices.

Beyond 1.3 GPa the quality of the single crystal deteriorated to such an extent that, by 1.9 GPa, no useful data could be obtained using single crystal diffraction methods. The behaviour of γ-glycine beyond this pressure was therefore investigated using synchrotron powder diffraction, the results obtained in that study (see below) indicate that the degradation of the single crystal of γ-glycine at pressure was due to a transformation to ε-glycine.

ε-Glycine

A single crystal of γ-glycine was gently crushed, rather than ground, and introduced into a Merrill-Bassett cell; during preparation of this sample every effort was taken not to place the material under mechanical stress, and this led to imperfect powder averaging in the sample. All lines in the powder pattern collected at ambient pressure were attributable to γ-glycine (Figure 3*a*). The patterns became markedly broader with increasing pressure, but they are consistent with almost conversion to a different phase at 4.3 GPa (Fig. 3*b,c*).

Boldyreva and co-workers have recently investigated the compression of γ-glycine in a study which is similar to the one described here.[32] A powder pattern obtained at 7.85 GPa was indexed on a primitive monoclinic unit cell of dimensions a = 4.780(1), b = 5.557(1), c = 5.379(1) Å, β = 118.25(1)° (note that we have swapped the original a and c axes to match those of the other phases described in this paper).

A structure of ε-glycine was proposed[32] on the basis of the powder diffraction measurements. The coordinates obtained in that study imply the presence of an N-H…O hydrogen bond in which the N…O separation is only 2.37 Å and non-H-bonded O…O contacts of 2.65 Å; the primary bond distances and angles also differed somewhat from typical ranges (*e.g.* the C-N bond measures 1.62 Å). These seem unusual, even for a structure derived at high pressure. We have obtained an alternative solution of the structure, which appears to fit our 4.3 GPa data (Figure 3*c*) somewhat better than the model proposed by Boldyreva (though, of course, the pressures used in the two studies are different). The indexing, space group and position of the molecules in the unit cell are the same as those used by Boldyreva; the two models differ in the orientations of the molecules. The shortest N-H…O hydrogen bond in our model has an N…O separation of *ca* 2.60 Å, which is at the lower limit of such distances observed under ambient conditions; the shortest O…O contacts measure 3.22 Å. These parameters are similar to those observed in serine at 5.3 GPa and α-glycine at 6.2 GPa. We note in passing that fitting the data obtained at 4.3 GPa to a model consisting of the δ and γ phases was inferior to the γ/ε model (*cf.* Figs. 3*b* and *c*).

The structure of ε-glycine consists of $C(5)$ chains of molecules formed by lattice repeats along **c**, and these are linked into a layer by lattice repeats along **a**, to build up $R^4_4(16)$ rings (Fig. 8*a*), which is similar to the same layer structure formed in α-glycine (*cf* Fig. 4*b*); this similarity is evident in the a, c and β cell dimensions for α-glycine at 6.2 GPa and ε-glycine at 4.3 GPa (see Table 1). The chains along **c** are formed by head-to-tail N1H3…O2 hydrogen bonds. At 4.3 GPa, the N…O separation in these chains is 2.81(4) Å, which compares to 2.740(7) Å in α-glycine at 6.2 GPa. The N1-H5…O1 contact, formed along **a**, which connects the chains into layers, is very short [2.59(4) Å].

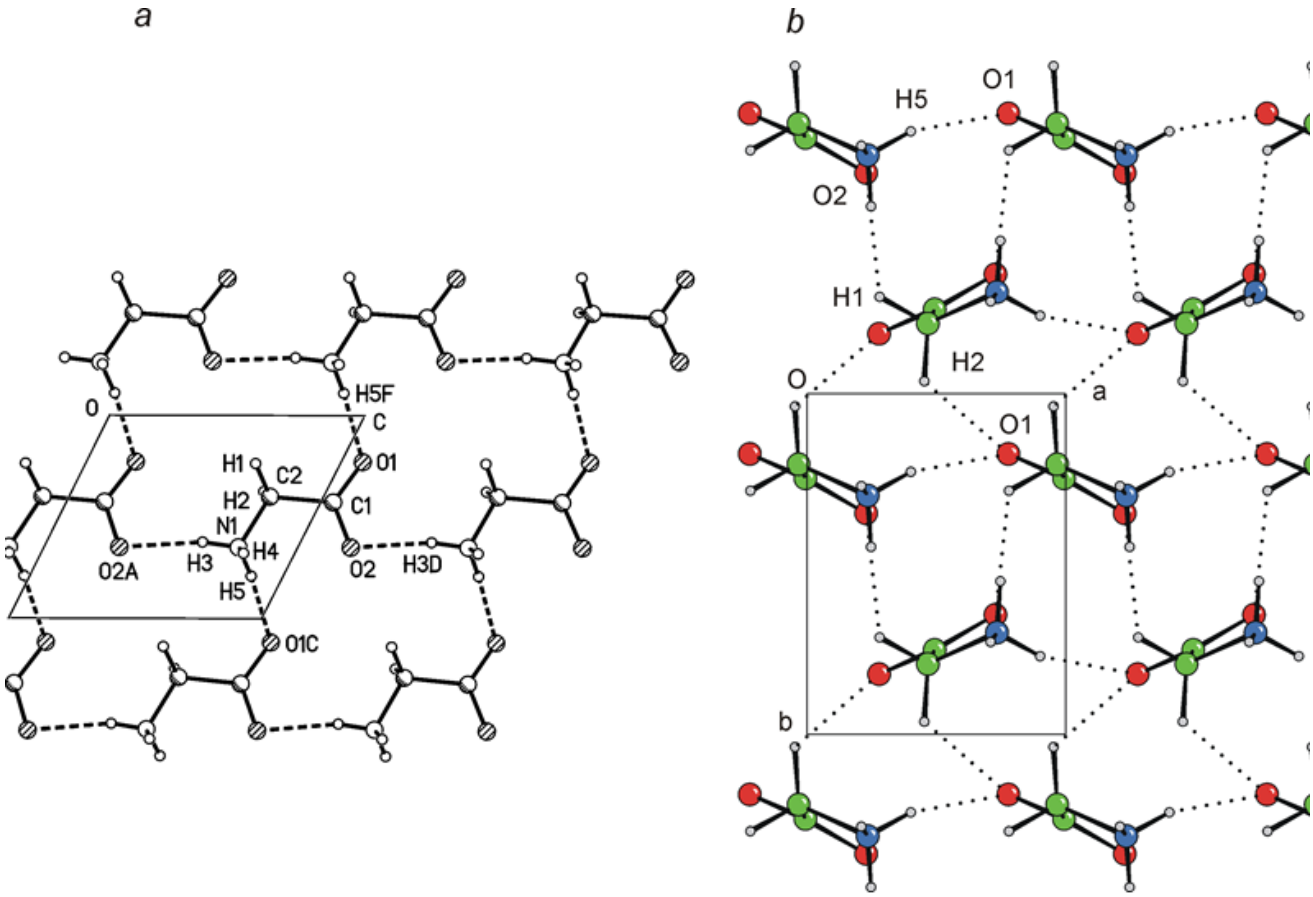

Figure 8. Hydrogen bonded layers (*a*) and layer stacking (*b*) in the crystal structure of ε-glycine at 4.3 GPa.

The layers are perpendicular to the *b*-axis, but not regularly spaced, so that they form a bi-layers structure reminiscent of that of α-glycine.[32] In ε-glycine the interlayer spacings are 2.38 and 3.38 Å. In α-glycine the closer pairs of layers are H-bonded together in interactions involving the H-atom which is not incorporated into the $R^4_4(16)$ ring network which forms the layers. Interestingly, in ε-glycine this atom (H4) is not involved in close H-bonding contacts, and the shortest contact involving H4 is formed across an N1…O1 vector with a distance of 3.15(5) Å. The shortest H…O interactions appear to be C2-H1…O2 contacts in which the C…O and H…O distances are 2.77(4) and 2.20(5) Å, respectively. Interatomic interactions spanning the larger inter-plane distance take the form of C2-H2…O1 interactions in which the C…O and H…O distances measure 3.05(5) and 2.36(5) Å, respectively.

These results were based on pressure-broadened powder diffraction data, and some caution needs to be exercised when interpreting them. But if our analysis is correct, this structure of ε-glycine suggests that application of pressure has led to the replacement of N-H…O hydrogen bonds by C-H…O hydrogen bonds. A more definitive study of this phase, possibly using neutron diffraction, would be highly desirable. We note,

however, that both our and Boldyreva's models are in agreement in that ε-glycine consists of irregularly-spaced α-glycine-like layers.

Comparison of the topologies of α, β, γ, δ and ε-glycine.

The coordination environment of a molecule in a crystal structure can be visualized using a Voronoi-Dirichlet polyhedron or VDP.[69,70] Voronoi-Dirichlet analysis is a method for partitioning space amongst points which occupy that space. A point is separated from a neighbouring point by a plane which bisects the vector between them. This construction is repeated for every pair of points to yield a subdivision of the space into cells which each contain one point. A convex VDP which characterizes the topology of packing in a crystal structure can be constructed using only the molecular centroids, the result is called a *lattice* VDP. The number of faces of the lattice VDP is called *the molecular packing number*, and is a kind of molecular coordination number. The number of molecules in the first, second and subsequent coordination shells defines the *coordination sequence*.

The coordination sequence of all five polymorphs of glycine is 14-50-100, which makes the structures topologically similar to body-centred cubic packing. The α, β, δ and ε polymorphs are all distorted from perfect BCC, but that of γ-glycine is particularly regular. Views of the first 14-centroid coordination shell of each polymorph are shown in Figure 9. The orientations of the structures in Figure 9 are along [001], which corresponds to the direction along the *C*(5) chains built from N1-H3…O2 hydrogen bonds (Figure 4*a*); this motif is observed in all five polymorphs.

Although the three ambient pressure polymorphs of glycine resemble each other topologically, there are differences in the relative senses in the directions of neighbouring *C*(5) chains (indicated in Figure 9 by + and – symbols). The topology of the molecular centroids and the senses of the C(5) chains in δ-glycine closely resemble those in β-glycine, and the ability of this transition to occur from one single crystal to another is readily understandable. The topologies of γ and ε-glycine are also very similar. However, comparison of Figs. 7 and 8 shows that during the transition of γ to ε glycine greater reorientation of the molecules takes place than in the β-to-δ transition. This, perhaps, explains why this phase transition does not proceed from one single crystalline form to the other.

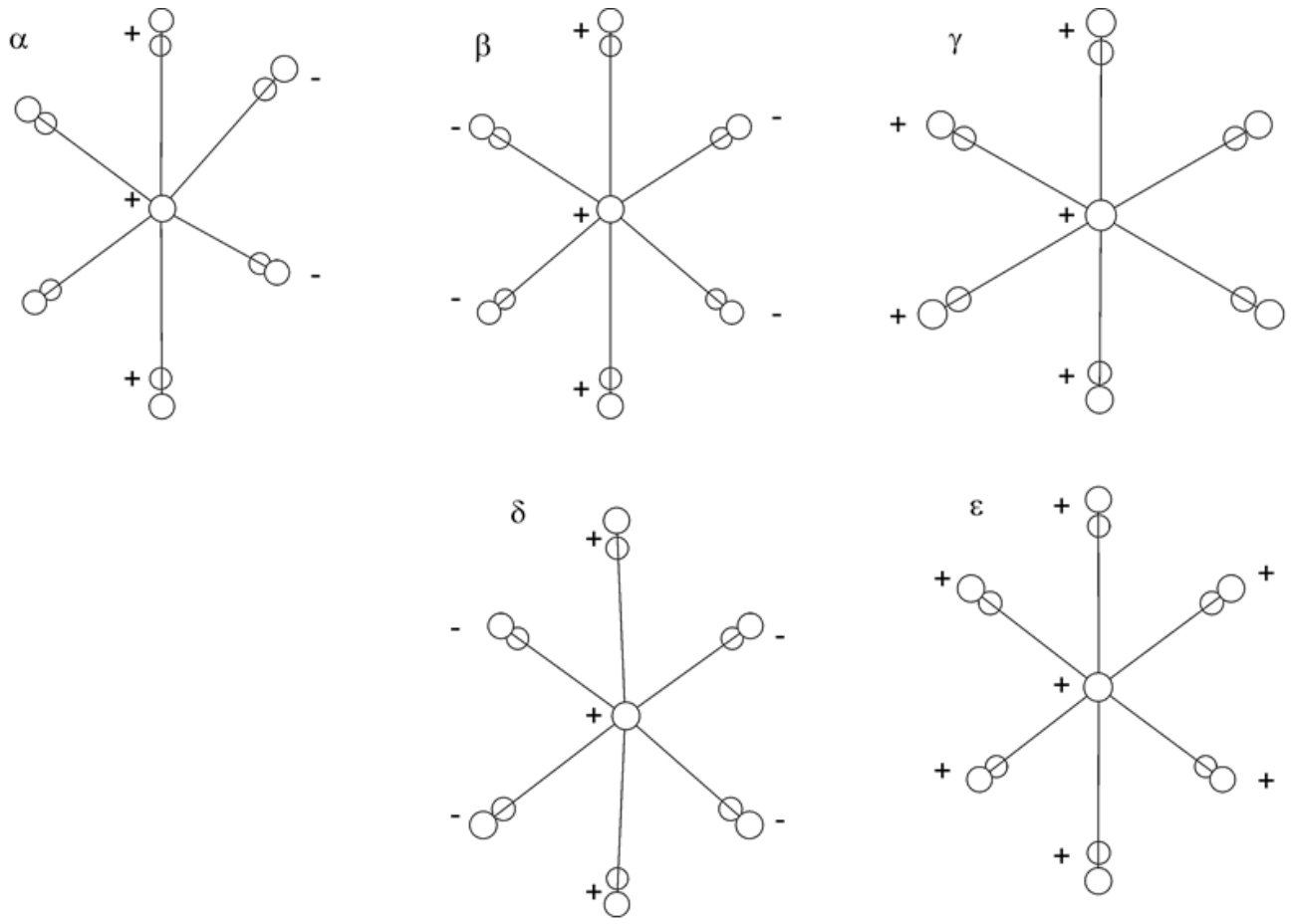

Figure 9. Topology of the molecular centroids in α, β, γ, δ and ε glycine. All views are along the *c*-axis in the directions of the chains shown in Figure 4*a*. The + and - symbols indicate the sense of the chain direction: '+' and '-' respectively mean that the ammonium or carboxylate groups point up out of the page. Note the similarity of the topologies and chain directions in the β and δ and in the γ and ε polymorphs.

Conclusions

We have shown that the behaviour of glycine depends on the identity of the starting polymorph, though similar factors appear to govern the response to high pressure of different forms. The α-form is stable to 23 GPa, and we have obtained a structure at 6.2 GPa. The principal effects of pressure to 6.2 GPa are to close-up voids which exist in the hydrogen-bonded layer structure by shortening CH…O hydrogen bonds which are present under ambient conditions, and the creation of new CH…O interactions. Conventional NH…O hydrogen bonds formed across the voids also shorten significantly, but others are left relatively unchanged.

The same comments can be applied to the effect that pressure has on the crystal structure of β-glycine, but in this case the system undergoes a single-crystal to single-crystal phase transition to a new polymorph (δ-glycine) at between 0 and 0.8 GPa. This has the effect of increasing the density of the sample substantially,

and there is an increase in the number of CH…O hydrogen bonds formed. The shortening of non-bonded interaction distances also characterizes the response of γ-glycine to high pressure, though this form is stable to about 2 GPa, where it transforms to ε-glycine. γ-Glycine does not display any significant degree of CH…O bonding, and so the γ to δ transition can be also viewed as forming a structure which is richer in this type of interaction, which, moreover, appears to be formed at the expense of NH…O interactions. This latter conclusion is based on a refinement against pressure-broadened powder data and a more definitive study is desirable. When studied using single crystal methods, the γ to ε transition causes break-up of the sample.

The differing behaviour of the polymorphs with respect to pressure can be traced to the orientational relationship between the molecules before and after the phase transition – these are very similar in the β and δ and γ and ε polymorphs,but quite different in the α-form.

The hydrogen bond distances observed in this study have O…N distances in the range 2.6 – 3.1 Å; these do not fall outside the range observed for structures determined under ambient conditions. This suggests that super-short hydrogen bonds are not formed at pressures below about 10 GPa, and this tentative conclusion is supported by our recent studies of other amino acids. Hydrogen bond distances do not necessarily decrease on application of pressure, and they may even increase; the effect of pressure on individual hydrogen bonds can be rationalized by other changes, such as closing-up of voids or CH…O bond formation, which occur under compression. Similar conclusions were derived after a recent study on the effect of pressure on L-serine.

The data derived in this study are likely to be useful in the derivation of pressure-dependent potential functions for amino acid residues. These in turn will allow the effect of pressure on proteins to be probed computationally. But as well as providing what we hope prove to be useful data for molecular modelling studies, we have also demonstrated that high-pressure is a versatile tool for the study of polymorphism. This is well-known to mineralogists and condensed matter physicists, though so far there have been relatively few studies of more complex molecular systems.

Notes and references

[1] Hemley, R.J.; Dera, P. *Rev. Mineral. Geochem.*, **2000**, *41*, 335 and references cited therein.

[2] Boldyreva, E.V. *J. Mol. Struct.* **2004**, *700*, 151 and references cited therein.

[3] Fourme, R.; Kahn, R.; Mezouar, M.; Girard, E.; Hoerentrup, C.; Prange, T. Ascone, I. *J. Synchrotron Rad.* **2001**, *8*, 1149.

[4] Girard, E.; Kahn, R.; Ascone, I.; Mazouar, M.; Dhaussy, A.-C.; Lin, T.; Johnson, J.E.; Fourme, R. *High Pressure Res.* **2004**, *24*, 173.

[5] Fourme, R.; Ascone, I.; Kahn, R.; Mezouar, M.; Bouvier, P.; Girard, E.; Lin, T.; Johnson, J.E. *Structure* **2002**, *10*, 1409.

[6] Kwon, O.Y.; Kim, S.Y.; No, K.T.; Kang, Y.K.; Jhon, M.S.; Scheraga, H.A. *J. Phys. Chem.* **1996**, *100*, 17670.

[7] Kyoung, T.N.; Kwon, O.Y.; Kim, S.Y.; Cho, K.H.; Yoon, C.N.; Kang, Y.K.; Gibson, K.D.; Jhon, M.S.; Scheraga, H.A. *J. Phys. Chem.* **1995**, *99*, 13019.

[8] Engh, R.A.; Huber, R. *Acta Crystallogr. A*, **1991**, *47*, 392.

[9] Moggach, S.A.; Allan, D.R.; Morrison, C.A.; Parsons, S.; Sawyer L. *Acta Cryst. B,* **2005**,*61*, 58.

[10] *a*. Murli, C.; Sharma, S.M; Karmakar, S.; Sikka, S.K. *Physica B* **2003**, *339*, 23. *b*. Goryainov, S.V.; Kolesnik, E.N.; Boldyreva, E.V. *Physica B* **2005**, *357*, 340.

[11] Moreno, A.J.D.; Freire, P.T.C.; Melo, F.E.A.; Araujo Silva, M.A.;Guedes, I.; Mendes Filho, J. *Solid State Commun.* **1997**, *103*, 655.

[12] Teixeira, A.M.R.; Freire, P.T.C.; Moreno, A.J.D.; Sasaki, J.M.; Ayala, A.P.; Mendes Filho, J.; Melo, F.E.A.; *Solid State Commun.* **2000**, *116*, 405.

[13] Moggach, S.; Parsons, S.; Allan, D.R. 22nd European Crystallographic Meeting, Budapest, Hungary, 26-31 August, 2004.

[14] Albrecht, G.; Corey, R.B. *J. Amer. Chem. Soc.* **1939**, *61*, 1087.

[15] *a.* Marsh, R.E. *Acta Crystallogr.* **1958**, *11*, 654. *b*. Destro, R.; Roversi, P.; Barzaghi, M.; Marsh, R.E. *J. Phys. Chem A* **2000**, *104*, 1047.

[16] *a*. Jönsson, P.-G.; Kvick, Å. *Acta Crystallogr. B* **1972**, *28*, 1827. *b.* Power, L. F.; Turner, K. E.; Moore, F. H. *Acta Crystallogr. B* **1976**, *32*, 11.

[17] Legros, J.-P.; Kvick, Å. *Acta Crystallogr. B* **1980**, *36*, 3052.

[18] Boldyreva, E.V.; Drebushchak, T.N.; Shutova, E.S. *Z. Krist.* **2003**, *218*, 366.

[19] Pervolich, G.L.; Hansen, L.K.; Bauer-Brandl, A. *J. Therm. Anal. Calorimetry* **2001**, *66*, 699.

[20] *a*. Iitaka, Y. *Proc. Jap. Acad.* **1954**, *30*, 109. *b*. Iitaka, Y. *Acta Crystallogr.* **1961**, *14*, 1.

[21] Kvick, Å.; Canning, W.M.; Koetzle, T.F.; Williams, G.J.B. *Acta Crystallogr. B* **1980**, *36*, 115.

[22] Zaccaro, J.; Matic, J.; Myerson, A.S.; Garetz, B.A. *Cryst. Growth Des.* **2001**, *1*, 5.

[23] Oxtoby, D.W. *Nature* **2002**, *420*, 277.

[24] Garetz, B.A.; Matic, J.; Myerson, A.S. *Phys. Rev. Lett.* **2002**, *89*, 175501.

[25] Gidalevitz, D.; Feidenhans'l, R.; Matlis, S.; Smilgies, D.-M.; Christensen, M.; Leiserowitz, L. *Angew. Chem. Int. Ed. Engl.* **1997**, *36*, 955.

[26] Iitaka, Y. *Acta Crystallogr.* **1960**, *13*, 35.

[27] Chongprasert, S.; Knopp, S.A.; Nail, S.L. *J. Pharm. Sci.* **2001**, *90*, 1720.

[28] Park, K.; Evans, J.M.B.; Myerson, A.S. *Cryst. Growth Des.* **2003**, *3*, 991.

[29] Sakai, H.; Hosogai, H.; Kawakita, T.; Onuma, K.; Tsukamoto, K. *J. Cryst. Growth* **1992**, *116*, 421.

[30] Ferrari, E.S.; Davey, R.J.; Cross, W.I.; Gillon, A.L.; Towler, C.S. *Cryst. Growth Des.* **2003**, *3*, 53.

[31] Boldyreva, E.V.; Ahsbahs, H.; Weber, H.-P. *Z. Krist.* **2003**, *218*, 231.

[32] Boldyreva, E.V.; Ivashevskaya, S.N.; Sowa, H.; Ahsbahs, H.; Weber, H.-P. *Doklady Phys. Chem.* **2004**, *396*, 111.

[33] Dawson, A. *PhD Thesis*. The University of Edinburgh, 2003.

[34] *a*. Desiraju, G.R.; Steiner, T. *The Weak Hydrogen Bond*. IUCr Monographs on Crystallography No. 9. Oxford University Press, Oxford, UK, 1999. *b*. Steiner, T. *Angew. Chem.Int. Ed.* **2002**, *41*, 48. *c*. Castellano, R.K. *Curr. Org. Chem.* **2004**, *8*, 845.

[35] Jeffrey, G.A.; Maluszynska, H. *Int. J. Biol. Macromol.* **1982**, *4*, 173.

[36] Derewenda, Z.S.; Lee, L.; Derewenda, U. *J. Mol. Biol.* **1995**, *252*, 248.

[37] Hummer, G.; Garde, S.; Garcia, A.E.; Paulaitis, M.E.; Pratt, L.R. *Proc. Nat. Acad. Sci. USA* **1998**, *95*, 1552.

[38] Merrill, L.; Bassett, W.A. *Rev. Sci. Instrum.*, **1974**, *45*, 290.

[39] Miletich, R.; Allan, D.R.; Kuhs, W.F. . *Mineral. Geochem.*, **2000**, *41*, 445.

[40] Piermarini, G. J.; Block, S.; Barnett, J. D.; Forman, R. A. *J. Appl. Phys.* **1975**, *46*, 2774.

[41] Cernik, R.J.; Clegg, W.; Catlow, C.R.A.; Bushnell-Wye, G.; Flaherty, J.V.; Greaves, G.N.; Burrows, I.; Taylor, D.J.; Teat, S.J.; Hamichi, M. *J. Synchrotron Rad.* **1997**, *4*, 279

[42] Dawson, A.; Allan, D.R.; Clark, S.J.; Parsons, S.; Ruf, M. *J. Appl. Crystallogr.* **2004**, *37*, 410.

[43] Bruker-AXS (2003). SAINT version 7. Bruker-AXS, Madison, Wisconsin, USA.

[44] Parsons, S. *SHADE*. Program for empirical absorption corrections to high pressure data. The University of Edinburgh, Scotland, 2004.

[45] Sheldrick, G. M. *SADABS.* Bruker-AXS, Madison, Wisconsin, USA., 2004.

[46] Betteridge, P.W.; Carruthers, J.R.; Cooper, R.I.; Prout, K.; Watkin, D.J. *J. Appl. Crystallogr.* **2003**, *36*, 1487.

[47] Sheldrick, G. M. *XP.* Bruker-AXS, Madison, Wisconsin, USA., 1997.

[48] Watkin, D. J., Pearce, L. & Prout, C. K. *CAMERON.* A Molecular Graphics Package. Chemical Crystallography Laboratory, University of Oxford, England, 1993.

[49] Bruno, I.J.; Cole, J.C.; Edgington, P.R.; Kessler, M.; Macrae, C.F.; McCabe, P.; Pearson, J.; Taylor, R. *Acta Crystallogr*. *B* **2002**, *58*, 389.

[50] Spek, A. L. *PLATON. A Multipurpose Crystallographic Tool*, Utrecht University, Utrecht, The Netherlands, 2004.

[51] Farrugia, L. J. *J. Appl. Crystallogr.* **1999**, *32*, 837.

[52] *a*. Hazen, R.M.; Finger, L.W. *Comparative Crystal Chemistry*, John Wiley & Sons, Chichester, 1982, page 81. *b.* Press, W.H.; Teukolsky, S.A.; Vetterling, W.T.; Flannery, B.P. *Numerical Receipes in Fortran*, Second Edition, Cambridge University Press, Cambridge, England, 1992. Subroutine *JACOBI*.

[53] Blatov, V.A.; Shevchenko, A.P.; Serezhkin, V.N. *J. Appl. Crystallogr.* **2000**, *33*, 1193.

[54] Allen, F.H. *Acta Crystallogr. B* **2002**, *58*, 380.

[55] Allen, F. H.; Motherwell, W. D. S. *Acta Crystallogr*. *B* **2002**, *58*, 407.

[56] Makarov, E.S.;Tobelko, K.I. *Doklady Akademii Nauk SSSR* **1984**, *275***,** 91.

[57] Sheldrick, G.M. *SHELXS*, University of Göttingen, Germany, 2001.

[58] Nelmes, R.J.; McMahon, M.I. *J. Synchrotron Rad.* **1994**, *1*, 69.

[59] Piltz, R.O.; McMahon, M.I.; Crain, J.; Hatton, P.D.; Nelmes, R.J.; Cernik, R.J.; Bushnell-Wye, G. *Rev. Sci. Instrum.* **1992**, *63*, 700.

[60] Coelho, A. Topas-A: General Profile and Structure Analysis Software for Powder Diffraction Data. 2005.

[61] Young, R.A. (Ed.) *The Rietveld Method.* IUCr Monographs on Crystallography No 5. Oxford University Press, Oxford, UK, 1993.

[62] Järvinen, M. *J. Appl. Crystallogr.* **1993**, *26*, 525.

[63] Dollase, W.A. *J. Appl. Crystallogr.* **1986**, *19*, 267.

[64] Pawley, G.S. *J. Appl. Cryst.* **1981**, *14*, 357.

[65] David, W.I.F.; Shankland, K.; McCusker, L.B.; Baerlocher, C. (Eds.) *Structure Determination from Powder Diffraction Data.* IUCr Monographs on Crystallography No. 13. Oxford University Press, Oxford, England. 2002.

[66] A review on graph set notation is given in: Bernstein, J.; Davis, R.E.; Shimoni, L; & Chang, N-L. *Angew. Chem. Int. Ed. Engl*. **1995**, *34*, 1555.

[67] A second interaction N1-H5…O2 is formed in which the N1…O2 distance is actually shorter [2.9516(11) Å] than in the N1-H5…O1 H-bond [3.0748(11) Å]. However, the angle formed at hydrogen is only 115.7(15)°, and the H5…O2 distance [2.415(19) Å] is *longer* than H5…O1 [2.183(15)Å]; this interaction is usually considered to be a van der Waals contact. This illustrates a potential pit-fall in considering only interactions between non-hydrogen atoms in the analysis of H-bonded structures.

[68] Cambridge Database default values for typical C-H and N-H bond distances are 1.083 and 1.009 Å, respectively. See also Reference 34*a*, page 8.

[69] Peresypkina, E.V.; Blatov, V.A. *Acta Crystallogr. B*, **2000**, *56*, 501.

[70] Peresypkina, E.V.; Blatov, V.A. *Acta Crystallogr. B*, **2000**, *56*, 1035-1045.